International Journal of Applied Science and Engineering
2008. 6, 2: 111-139

Comparative Performance of Isolation Systems for Benchmark Cable-stayed Bridge

Purnachandra Saha and R. S. Jangid*

Department of Civil Engineering
Indian Institute of Technology Bombay, Powai, Mumbai-400 076, India.

Abstract: Earthquake response of benchmark cable-stayed bridge with different isolation systems is investigated. The selected isolation system consists of high damping rubber bearing (HDRB), lead-rubber bearing (LRB), friction pendulum system (FPS) and resilient-friction base isolator (R-FBI). Considering the phase-I benchmark problem, the ground acceleration is only applied in the longitudinal direction acting simultaneously at all supports. The seismic response of the benchmark bridge is obtained by solving the governing equations of motion of bridge by Newmark's step-by-step integration method. A comparative performance study among the selected isolators for seismic response control of bridge is carried out. A parametric study for investigating the effectiveness is also performed with variation of important isolator parameters. Varying the different parameters of the isolators, evaluation criteria of the benchmark cable stayed bridge problem are found out. Significant reduction in base shear, overturning moment and other responses are observed by using the control systems by seismic isolator. Comparing the evaluation criteria of the benchmark problem, it is observed that the performance of LRB and R-FBI are better than that of the HDRB and FPS. Further, increase in the bearing damping ratio reduces both device displacement and base shear for HDRB and LRB. The effects of device isolation period on structure depend on the isolator as well as the type of selected input earthquake motion.

Keywords: Benchmark cable-stayed bridge; HDRB; LRB; FPS; R-FBI; seismic response; base isolation

1. Introduction

Cable-stayed bridges, which are very popular nowadays, are susceptible to strong earthquake motions because of the associated low damping and high flexibility. For direct comparison among the various control strategies for a particular type of structure, benchmark problems were generated so that the researcher can compare their various algorithms, devices and sensors for a particular structure through benchmark problem. Based on the Bill Emerson Memorial Bridge constructed in Cape Girardeau, Missouri, USA, benchmark problem on cable-stayed bridge have been generated [1]. Benchmark problem specified some performance objective from which direct comparison could be made.

There are several types of passive control devices used by various researchers to control the seismic response of the cable-stayed bridge. Ali and Abdel-Ghaffar [2] investigated the effectiveness of elastomeric bear-

* Corresponding author; e-mail: rsjangid@civil.iitb.ac.in *Accepted for Publication: December 27, 2008*

ings (both elastic and hysteretic types) for seismic isolation of cable-stayed bridges. They observed that a significant reduction in the seismic forces induced on bridges could be achieved through installation of the hysteretic energy dissipation types of devices at appropriate locations. Seismic retrofit of a cable-stayed bridge by employing rubber bearings and viscous dampers has been investigated by Iemura et al. [3]. From numerical simulation of an existing cable-stayed bridge in Japan, they observed that structural control strategies consisting of base isolation bearings and dampers can significantly reduce the structural responses incurred by earthquake ground motions. Lead-rubber bearings have been applied by Park et al. [4] in the phase-I benchmark cable-stayed bridge problem. It was observed that LRBs were effective in reducing the seismic forces induced on bridges, but, large deck displacement was caused by this control system. To obtain the additional reduction of seismic responses, the linear viscous dampers with LRBs are considered between the deck and the tower/abutment [5]. The results of this strategy are comparable to any control strategies (e.g., active, semi-active or hybrid) as it significantly reduces all evaluation criteria specified in the benchmark problem. Bontempi et al. [6] examined the response of the phase-I benchmark cable-stayed bridge with viscoelastic and elastoplastic dampers. It is observed from their numerical results, that viscoelastic damper is one of the best control strategies for phase-I benchmark control problem. They found that the passive system seems to be the most convenient among the control strategies. The advantages of passive system are that, it supplies values of internal action similar to the active system but availability of electric power supplies is not necessary and its realization is easier. He and Agrawal [7] investigated the effectiveness of passive linear viscous damper and observed that it significantly reduces bridge responses subject to near field earthquake motion with pulse period larger than fundamental period of the bridge. The parametric study of base-isolated structures considering elastomeric bearing and sliding systems has been carried out by Jangid [8] and found that isolation system parameters significantly influence the earthquake response of structure. The success of passive dampers for controlling the seismic forces leads us to study the performance of the different isolating systems for phase-I benchmark cable-stayed bridge. From the detailed literature review on the benchmark cable stayed bridge, it is observed that very little work has been carried out on the application of various isolation systems on benchmark cable stayed bridge and comparison of their performances. So there is a need to compare performance of various isolators and to investigate the effectiveness of the isolators.

The aim of the present study is to investigate the effectiveness of isolation systems (i.e., HDRB, LRB, FPS and R-FBI) for seismic response control of the benchmark cable-stayed bridge subjected to specified earthquake ground motions. The objectives of the study are (i) to investigate and compare the effectiveness of HDRB, LRB, FPS and R-FBI for seismic response control of the benchmark cable-stayed bridge, and (ii) to investigate the influence of variation in important parameters of the isolators on the response of the bridge.

2. Benchmark cable-stayed bridge

The benchmark problem definition and detailed description for cable-stayed bridge was developed by Dyke et al. [1]. The problem is based on Bill Emerson memorial Bridge as shown in Figure 1. The critical damping of the evaluation model is 3%. The important responses to be considered for a cable-stayed bridge subject to an earthquake in the longitudinal direction are (i) force responses of the towers, (ii) the displacement of the deck and (iii) the variations of force in the stays, which should be confined in the range $0.2T_f$ - $0.7T_f$ (with T_f denoting the failure tension) [1]. The bridge without control can assume two distinct evaluation models: (a) a model in which the deck is restrained longitudinally to the main piers by dynamically stiff shock transmission devices. The first ten frequencies of this configuration are 0.2899, 0.3699, 0.4683, 0.5158, 0.5812, 0.6490, 0.6687, 0.6970, 0.7120 and 0.7203 Hz [1]. The fundamental time period of this model is 3.43 sec. In this case, the bridge shows limited deck displacement (maximum 0.0975 m) but a high shear at the base of the towers as well as unacceptable variations of tension in the cables: (b) a model in which the deck is not restrained (shock transmission devices removed) longitudinally to the piers and the tie in this direction is supplied only by the cable stays. The first ten frequencies of this second configuration are 0.1618, 0.2666, 0.3723, 0.4545, 0.5015, 0.5650, 0.6187, 0.6486, 0.6965 and 0.7094 Hz [1]. In this model, even though maximum values of shear and moment respectively equal to 45.6 and 58.7% of those of model (a), there is an unacceptable sliding of the deck, with a maximum displacement equal to 0.77 m.

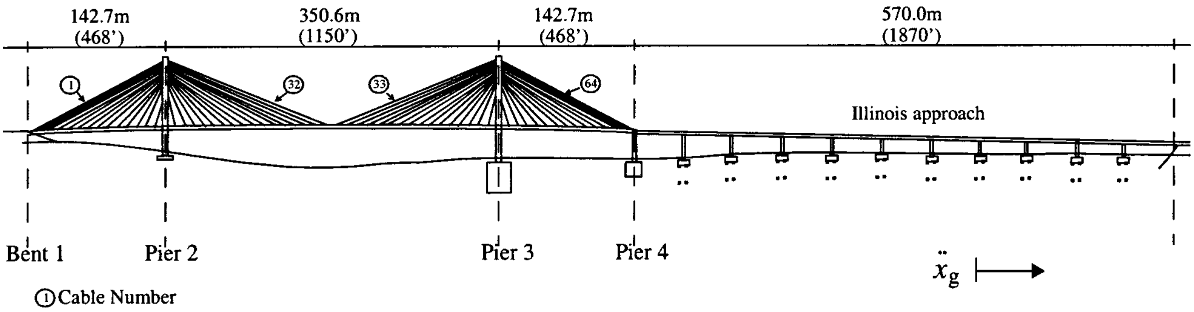

Figure 1. Schematic diagram of the Cape Girardeau Bridge.

There are 18 evaluation criteria mentioned in the benchmark problem [1] as listed in Tables. Among them, the first six evaluation criteria (J_1 to J_6) are related to peak responses of the bridge with respect to uncontrolled bridge (model (a)), where J_1 is the ratio of peak base shear of the towers, J_2 is the ratio of peak shear force at deck level of the towers, J_3 is the ratio of peak overturning moment of the towers, J_4 is the ratio of peak moment at deck level of the towers, J_5 is the ratio of peak deviation in the cable tension and J_6 is the ratio of peak displacement of the deck at abutment. The next five evaluation criteria (J_7 to J_{11}) related to norm responses of the bridge with respect to uncontrolled bridge (model (a)), where J_7 is the ratio of norm base shear of the towers, J_8 is the ratio of norm shear force at deck level of the towers, J_9 is the ratio of norm overturning moment of the towers, J_{10} is the ratio of norm moment at deck level of the towers, J_{11} is the ratio of norm deviation in the cable tension. The norm of a response $\|.\|$ is defined as

$$\|.\| \equiv \sqrt{\frac{1}{t_f}\int_0^{t_f}[.]^2\,dt} \tag{1}$$

where t_f is the time required for the structural response to attenuate.

The last seven evaluation criteria (J_{12} to J_{18}) are related to the requirement of the applied control systems. Among them J_{12}, J_{13} and J_{16} are applicable to passive control systems, where J_{12} is the ratio of peak control force and weight of the structure, J_{13} is the ratio of maximum device stroke and maximum deck displacement and J_{16} is the total number of control devices applied.

3. Seismic isolation systems

3.1. High damping rubber bearing (HDRB)

HDRB is one type of elastomeric bearing. This type of bearing consist of thin layers of high damping rubber and steel plates built in alternate layers as shown in Figure 2(a). The vertical stiffness of the bearing is several hundred times the horizontal stiffness due to the presence of internal steel plates. Horizontal stiffness of the bearing is controlled by the low shear modulus of elastomer while steel plates provides high vertical stiffness as well as prevent bulging of rubber. High vertical stiffness of the bearing has no effect on the horizontal stiffness. The damping in the bearing is increased by adding extra-fine carbon block, oils or resins and other proprietary fillers [9]. The dominant features of HDRB system are the parallel action of linear spring and viscous damping. The damping in the isolator is neither viscous nor hysteretic, but somewhat in between. The ideal force deformation behavior of the bearing is shown in Figure 2(a). The restoring force (f) developed in the bearing is given by

$$f = c_b \dot{x}_b + k_b x_b \tag{2}$$

where c_b is the damping and k_b is the stiffness of the HDRB system; $\dot{x}_b$ and x_b are the device velocity and displacement, respectively.

The isolation time period (T_b) and damping ratio (ξ_b) of the system are provided by selecting the damping and stiffness of the HDRB.

$$T_b = 2\pi \sqrt{\frac{m_d}{\sum k_b}} \tag{3}$$

$$\xi_\mathrm{b} = \frac{\sum \mathrm{c_b}}{2 m_d \omega_\mathrm{b}} \tag{4}$$

where m_d is the total mass of the deck; and $\omega_\mathrm{b} = 2\pi/T_b$ is the isolation frequency of the isolator.

3.2. Lead-rubber bearing (LRB)

This type of elastomeric bearings consist of thin layers of low damping natural rubber and steel plates built in alternate layers and a lead cylinder plug firmly fitted in a hole at its centre to deform in pure shear as shown in Figure 2(b). The LRB was invented in New Zealand in 1975 [10] and has been used extensively in New Zealand, Japan and United States. The steel plates in the bearing force the lead plug to deform in shear. This bearing provides an elastic restoring force and also, by selection of the appropriate size of lead plug, produces required amount of damping [11]. For the present study the model proposed by Wen [12] is used to characterize hysteretic behaviour of the LRB. The force deformation behaviour of the bearing is shown in Figure 2(b). The restoring force (f) developed in the isolator is given by

$$f = c_b \dot{x}_b + \alpha k_b x_b + (1-\alpha) F^y Z_x \tag{5}$$

where c_b and k_b are the viscous damping and initial stiffness of the bearing, respectively; $\dot{x}_b$ and x_b are the device velocity and displacement, respectively; F^y is the yield strength of the bearing; α is an index which represents the ratio of post to pre-yielding stiffness; and Z_x is the dimensionless hysteretic displacement component satisfying the following non-linear first order differential equation expressed as

$$q\dot{Z}_x = A\dot{x}_b - \beta|\dot{x}_b||Z_x||Z_x|^{n-1} - \tau\dot{x}_b Z_x^n \qquad (6)$$

where q is the yield displacement of the bearing. Dimensionless parameters A, β, τ and n are selected such that predicted response from the model closely match with the experimental results. The parameter n is an integer constant, which controls the smoothness of transition from elastic to plastic response. In the time history analysis, the hysteretic displacement component, Z_x at each time step is obtained by solving Equation (6) with the help of 4th order Runge-Kutta method. The LRB system is characterized by damping ratio (ξ_b) (defined in Equation (4)) normalized yield strength (F_0) and isolation time period (T_b) which are defined as

$$T_b = 2\pi\sqrt{\frac{m_d}{\sum \alpha k_b}} \qquad (7)$$

$$F_0 = \frac{\sum F^y}{W_d} \qquad (8)$$

where αk_b and F^y are the post yield stiffness and yield strength of the bearing, respectively, m_d and W_d are the total mass and weight of the bridge deck respectively. The other parameters of the LRB system which do not affect much the peak response are kept constant (i.e., q = 2.5 cm, β = τ = 0.5, A = 1 and n = 2).

3.3. Friction pendulum system (FPS)

The FPS is a frictional isolation system that combines a sliding action and a restoring force by geometry. The FPS isolator, shown schematically in Figure 2(c) has an articulated slider that moves on a stainless steel spherical surface [13]. As the slider moves over the spherical surface, it causes the supported mass to rise and provides the restoring force for the system.

The natural period of the FPS depends on the radius of curvature (r_c) of the concave surface. The natural period of vibration (T_b) of a rigid mass supported on FPS connections is determined from the pendulum equation

$$T_b = 2\pi\sqrt{\frac{r_c}{g}} \qquad (9)$$

where g is the acceleration due to gravity. The isolated period becomes active once the friction force level of the isolator is exceeded.

The ideal force deformation behavior of FPS is shown in Figure 2(c). The resisting force (f) provided by the system can be given by

$$f = k_b x_b + F_x \qquad (10)$$

where k_b is the bearing stiffness provided by virtue of inward gravity action at the concave surface; x_b is the device displacement; and F_x is the frictional force. The system is characterized by bearing isolation period (T_b) and friction coefficient (μ).

Engineering investigations for the response of multi storied shear type buildings and bridges isolated by sliding systems have been presented by Jangid [14]. The frictional force of the sliding system was represented by the conventional and hysteretic models to investigate the comparative performance and computational efficiency of the two models. Results of the investigation indicated that the conventional and hysteretic models of sliding systems yielded similar seismic response for isolated structures. Hence, here, the frictional force of the FPS is modelled using the theory proposed by Wen [12].

For this hysteretic model, the frictional force mobilised in the system can be given by

$$F_x = F_s Z_x \tag{11}$$

where F_s is the limiting frictional force; and Z_x is the dimensionless hysteretic displacement component satisfying Equation (6). The parameters q and n of Equation (6) are taken equal to 0.1 cm and 15 respectively keeping other parameters the same as those of LRB.

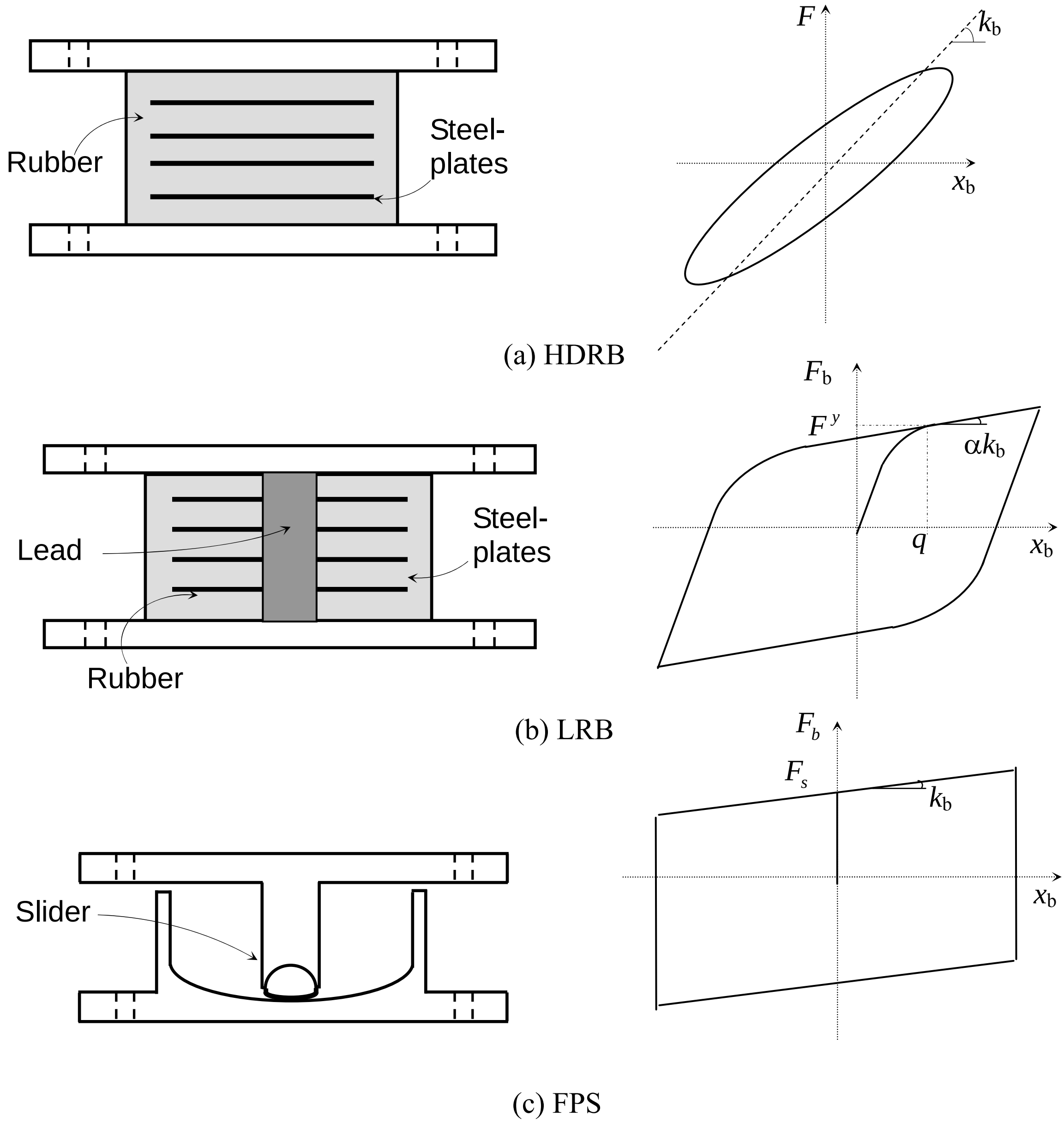

Figure 2. Schematic diagrams and ideal force-deformation behavior of the selected seismic isolation systems.

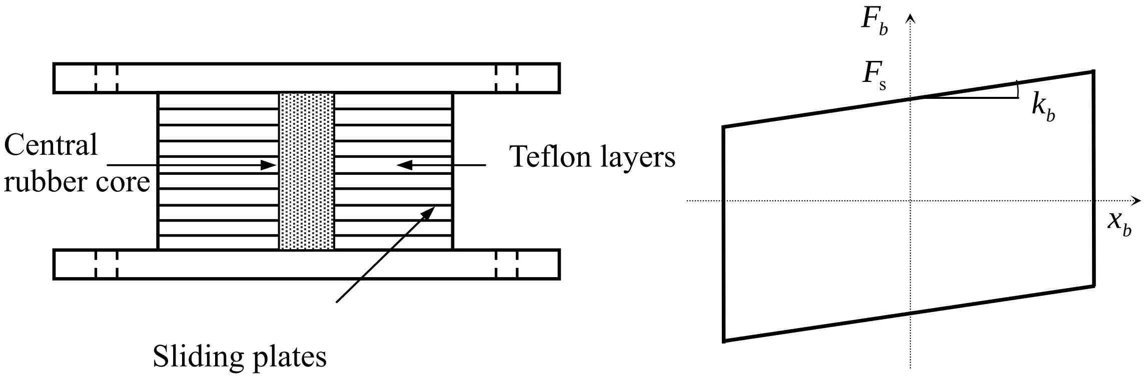

(d) R-FBI

Figure 2. Schematic diagrams and ideal force-deformation behavior of the selected seismic isolation systems.(continued)

3.4. Resilient-friction base isolators (R-FBI)

The R-FBI [15] is consist of a set of concentric layers of Teflon-coated plates in friction contact with each other with a central rubber core and/or peripheral rubber cores as shown in Figure 2(d). It combines the beneficial effect of friction damping with that of resiliency of rubber. The R-FBI provides isolation through the parallel actions of friction, damping and restoring force. The ideal force deformation behavior of R-FBI is shown in Figure 2(d). The resisting forces provided by the system can be given by

$$f = k_b x_b + c_b \dot{x}_b + F_x \qquad (12)$$

where k_b , c_b and F_x are the stiffness, damping and frictional force of the bearing respectively.

The parameters defining behavior of R-FBI system are the isolation period (T_b), damping ratio (ξ_b) and friction coefficient (μ). The T_b and ξ_b are evaluated from Equation (3) and (4), respectively. The limiting value of frictional force F_x of the system can be expressed by Equation (11). The frictional forces of the R-FBI are represented by continuous hysteretic model similar to that used for the FPS.

4. Governing equations of motion

The dynamic system of equations for a passively controlled structure can be written as

$$M\ddot{U} + C\dot{U} + KU = MG\ddot{x}_g + Nf \qquad (13)$$

in which **U** is the relative displacement vector; $\ddot{U}$ and $\dot{U}$ are the second and first time derivative of the response vector **U** respectively; **M** is the mass matrix; **C** is the damping matrix; **K** is the stiffness matrix; $\ddot{x}_g$ is the earthquake ground acceleration; **f** is the vector of the control forces; and **G** and **N** are the matrices of assignment that refer the seismic and control forces to the associated degree of freedom.

Figure 3 shows the SIMULINK [16] block for the seismic analysis of the passive control system.

5. Numerical study

A set of numerical simulation is performed in MATLAB [17] for the specified three historical earthquakes to investigate the effectiveness of the isolation systems. The fundamental frequency of the bridge in evaluation model (a) is 3.45 sec and that of evaluation model (b) is 6.18 sec. To implement the isolation systems, a total numbers of 24 isolators were used in 8 locations between the deck and pier/bent, 3 at each location. Since the fundamental frequency of the bridge in evaluation model (a) is around 3.5 sec, study has been carried out for the isolation time period of 3.5 sec for all the isolators. Time history analysis in longitudinal direction is performed for the three earthquake ground motions specified in the benchmark problem to obtain the structural responses of the bridge. The three specified earthquakes are: (1) 1940 El Centro NS with peak ground acceleration (PGA) equals to 0.35*g* and predominant frequency range (PFR) equals to 1.5 Hz; (2) 1985 Mexico City with PGA and PFR equals to 0.14*g* and 0.5 Hz respectively; (3) 1999 Gebze NS, Turkey which has PGA and PFR are equals to 0.27*g* and 2.0 Hz respectively. The design PGA value of the bridge is 0.36*g*. The time history and FFT of the above earthquakes are shown in Figure 4.

The time variation of the base shear response of the earthquakes for damping ratio of 15% for HDRB, 5% damping ratio and 0.1 normalized yield strength ratio (F_0) for LRB, 0.05 frictional coefficient for FPS while 10% damping ratio and 0.04 frictional coefficient for R-FBI are shown in Figures 5 to 8, respectively. The values of isolator parameters considered above are almost same as typical recommended values for these isolators [9]. From the figures, it can be observed that around 70% reduction for El Centro (1940) earthquake, 47% reduction for Mexico City (1985) earthquake and 60 to 66% reduction for Gebze (1999) earthquake can be achieved by these isolators. It can be noted that maximum reduction of base shear response in longitudinal direction, for El Centro (1940), Mexico City (1985) and Gebze (1999) earthquakes is achieved by R-FBI, FPS and HDRB respectively. LRB reduces the deck displacement effectively for all the specified earthquakes. The force-deformation behavior of the HDRB, LRB, FPS and R-FBI at pier 2 tower, for the earthquakes are shown in Figure 9. The evaluation criteria of the bridge considering the above isolation parameters are shown in Tables 1 to 3 for El Centro (1940), Mexico City (1985) and Gebze (1999) earthquakes, respectively. Table 4 shows the maximum values of the evaluation criteria for all the three earthquakes. From the results presented in Tables 1 to 4 and Figure 18, it can be deduced that isolation can substantially reduce the seismically induced forces in the bridge. Comparing the evaluation criteria Tables 1 to 4, it is observed that the performance of LRB is more consistent than the other isolators. Though FPS is observed better in controlling Mexico City (1985) earthquake responses, but considering all the three specified earthquakes it is found that the performance of R-FBI is better than that of HDRB and FPS.

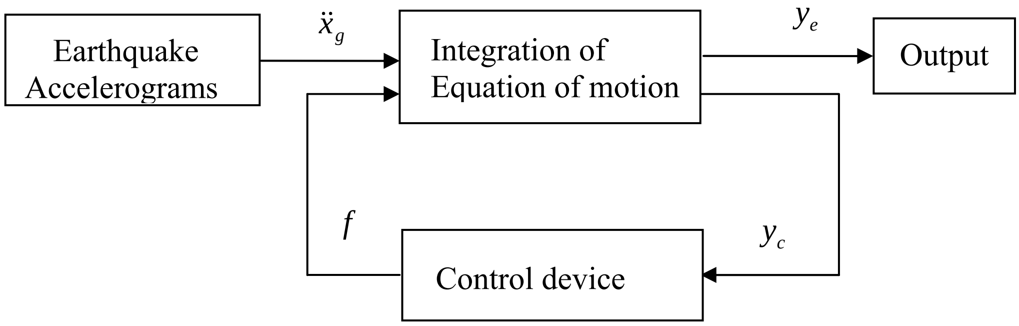

Figure 3. SIMULINK block diagram for passive control system.

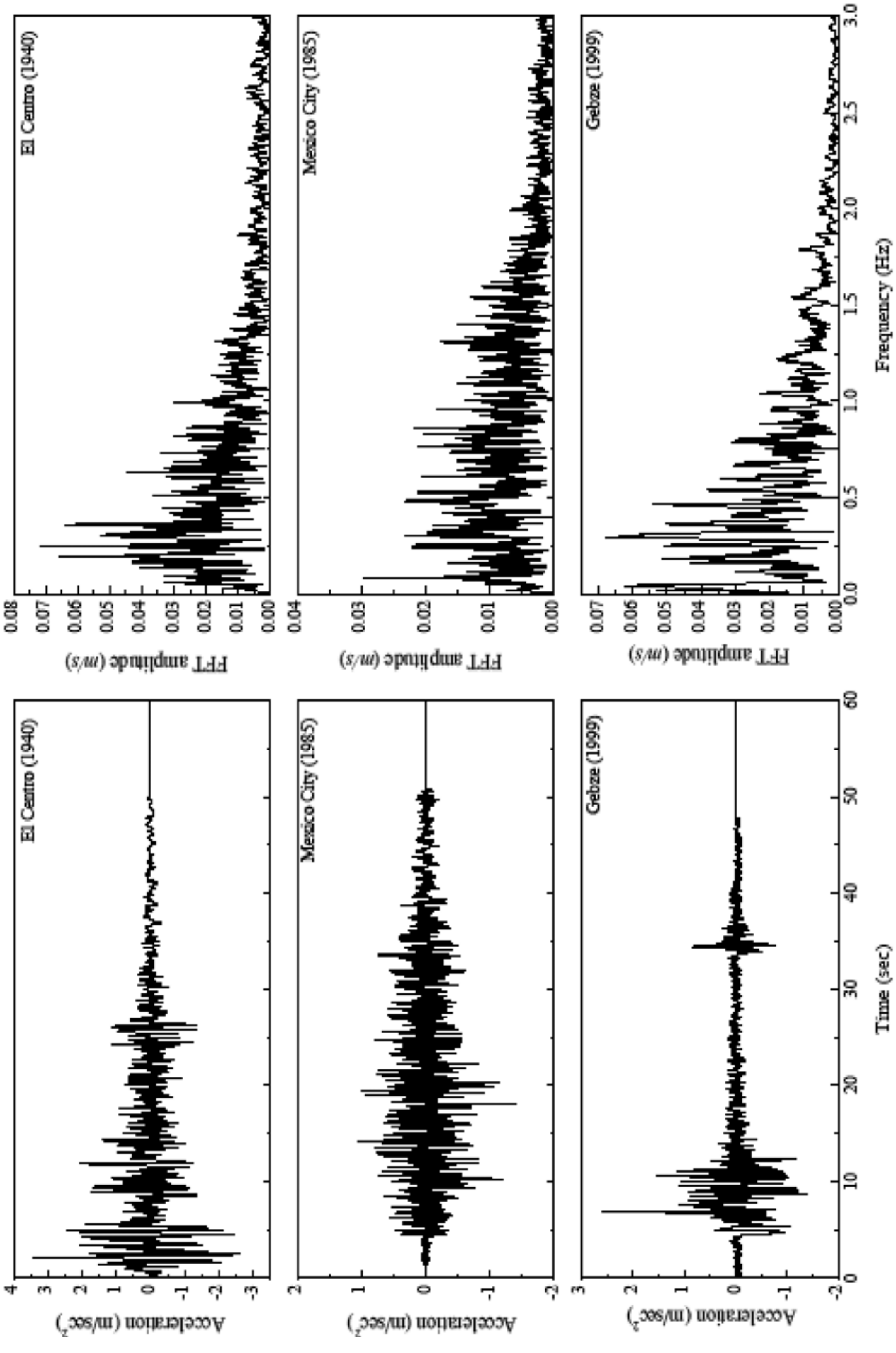

Figure 4. Time History and FFT of El Centro NS (1940), Mexico City (1985) and Gebze (1999) earthquakes respectively.

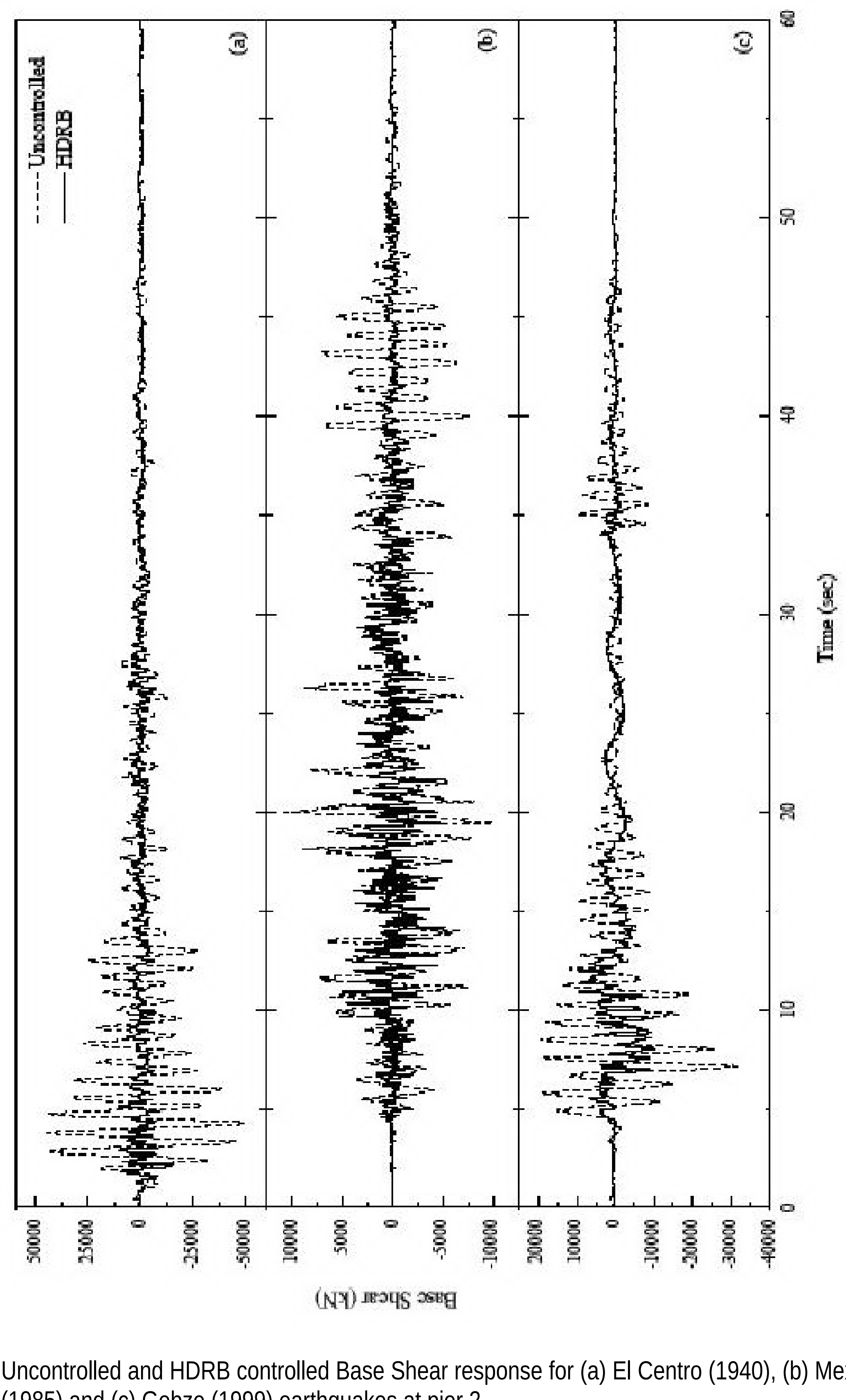

Figure 5. Uncontrolled and HDRB controlled Base Shear response for (a) El Centro (1940), (b) Mexico City (1985) and (c) Gebze (1999) earthquakes at pier 2.

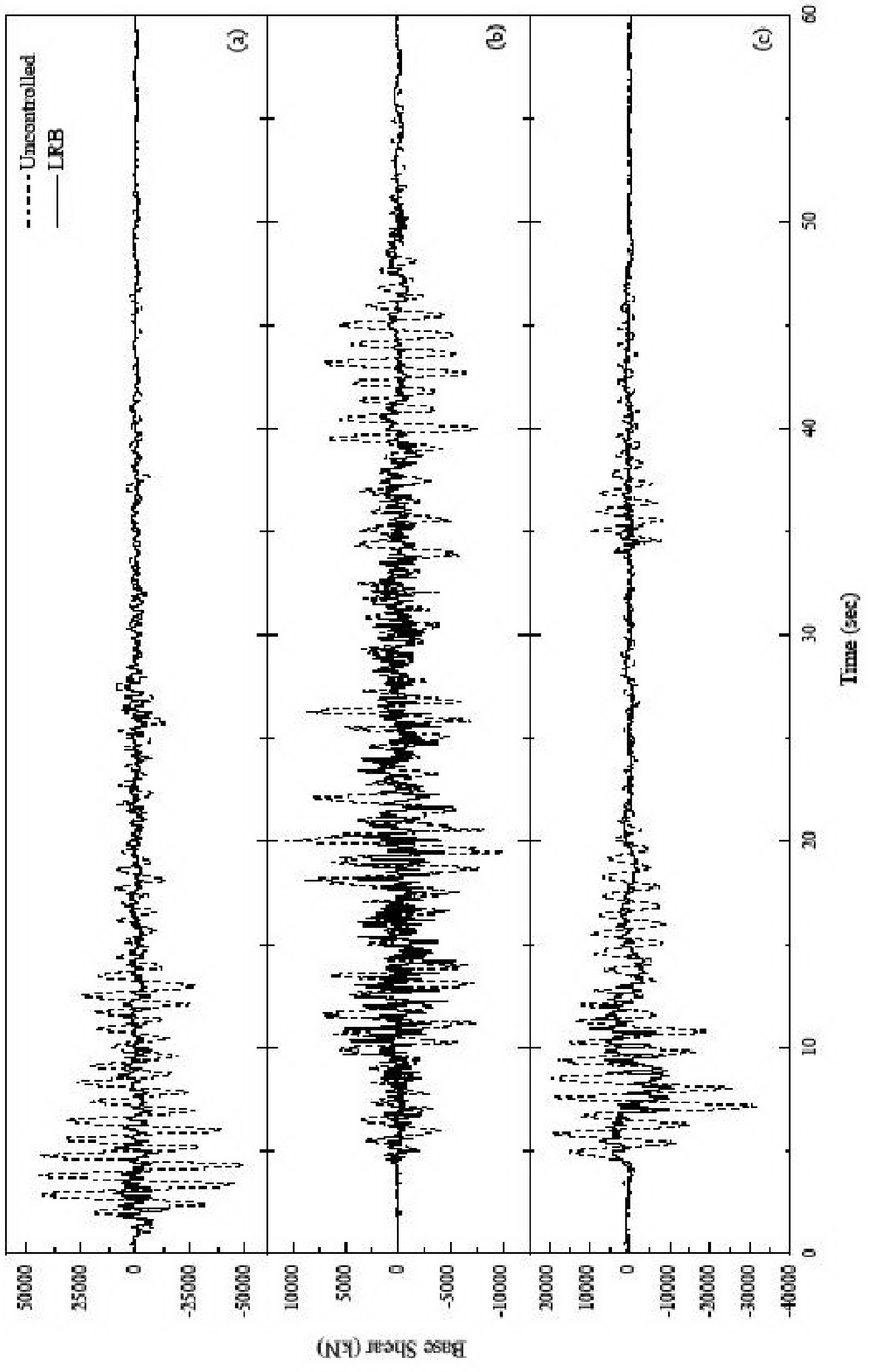

Figure 6. Uncontrolled and LRB controlled Base Shear response for (a) El Centro (1940), (b) Mexico City (1985) and (c) Gebze (1999) earthquakes at pier 2.

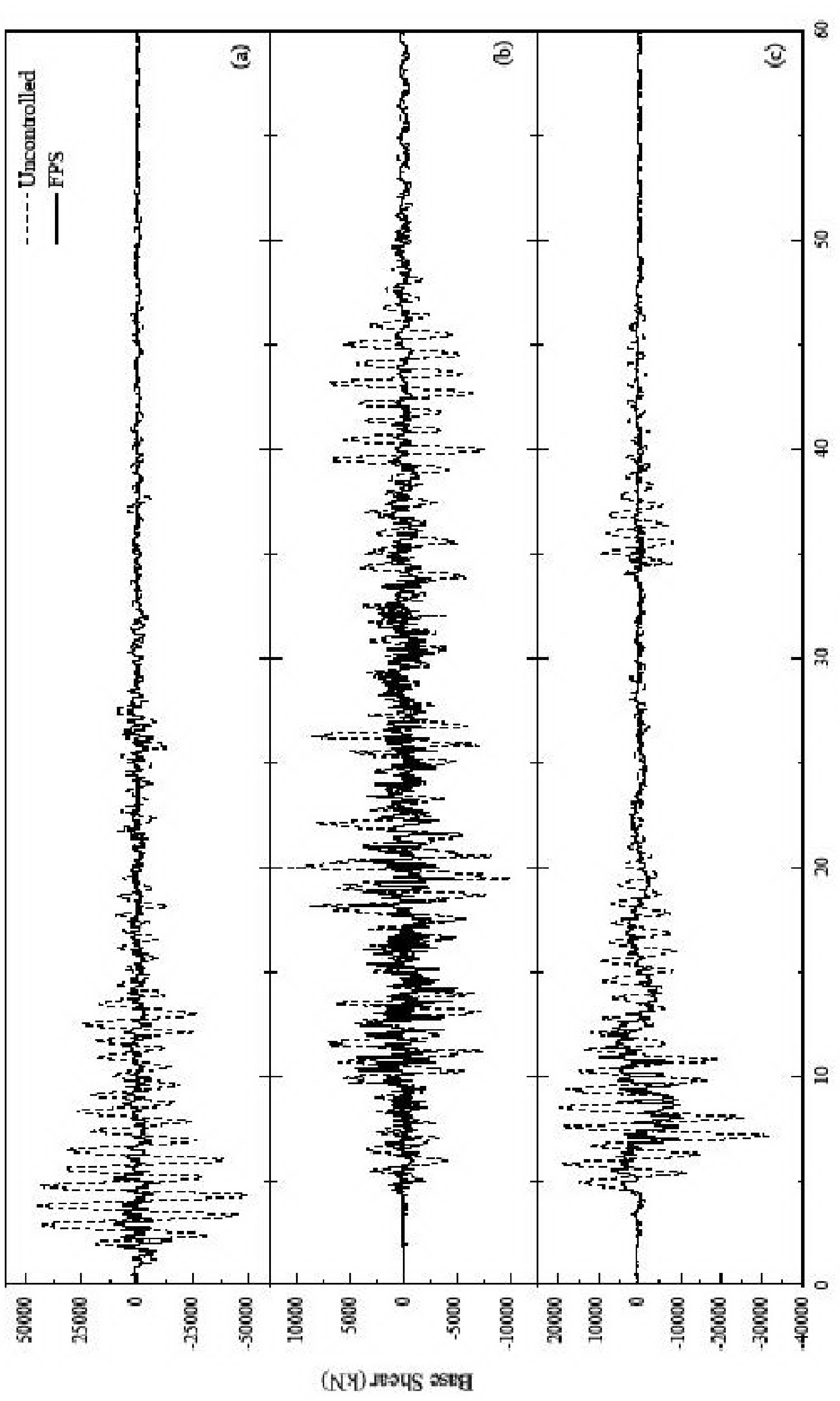

Figure 7. Uncontrolled and FPS controlled Base Shear response for (a) El Centro (1940), (b) Mexico City (1985) and (c) Gebze (1999) earthquakes at pier 2.

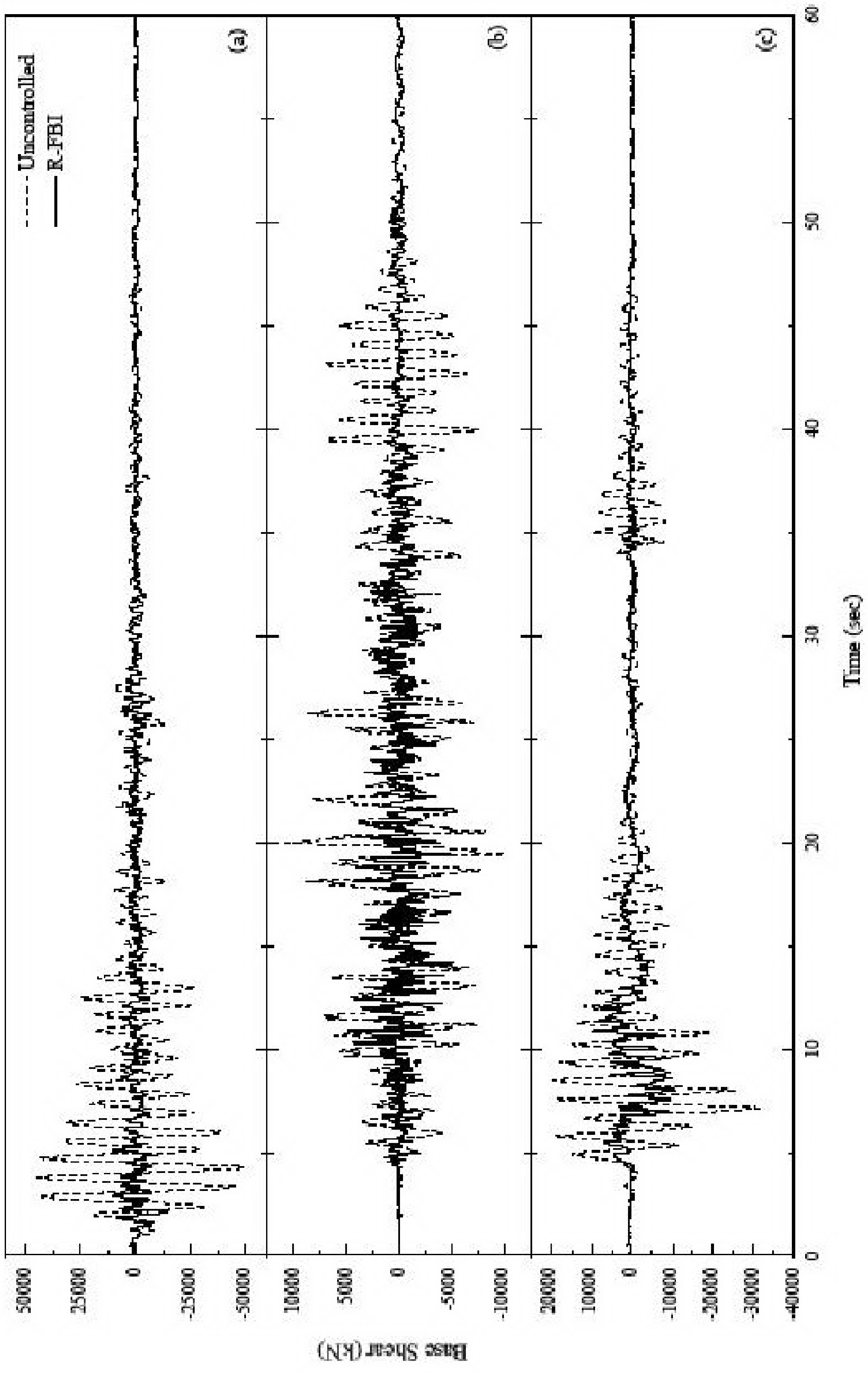

Figure 8. Uncontrolled and R-FBI controlled Base Shear response for (a) El Centro (1940), (b) Mexico City (1985) and (c) Gebze (1999) earthquakes at pier 2.

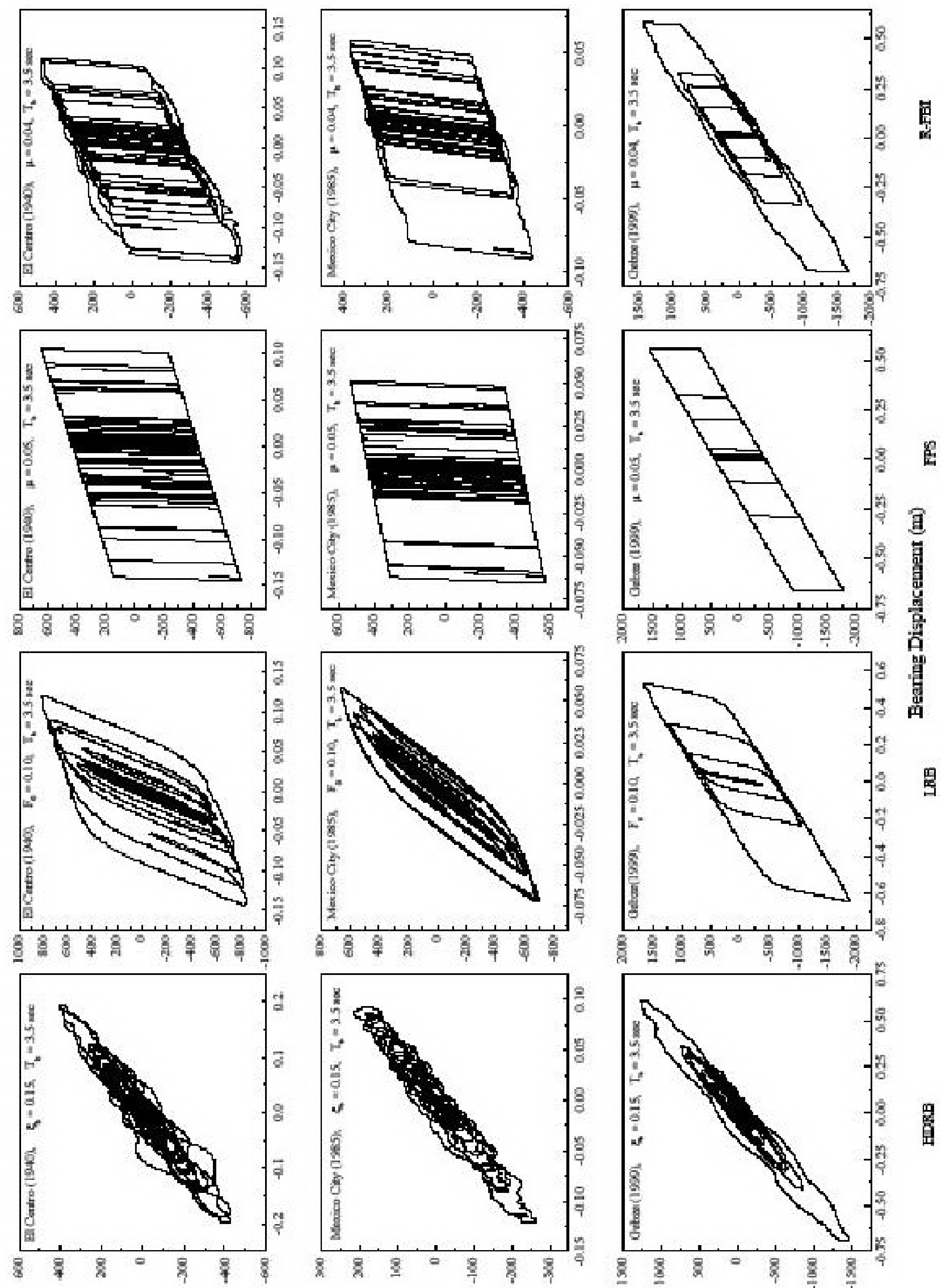

Figure 9. Force-deformation behavior of the HDRB, LRB, FPS and R-FBI for El Centro (1940), Mexico City (1985) and Gebze (1999) earthquakes at pier 2.

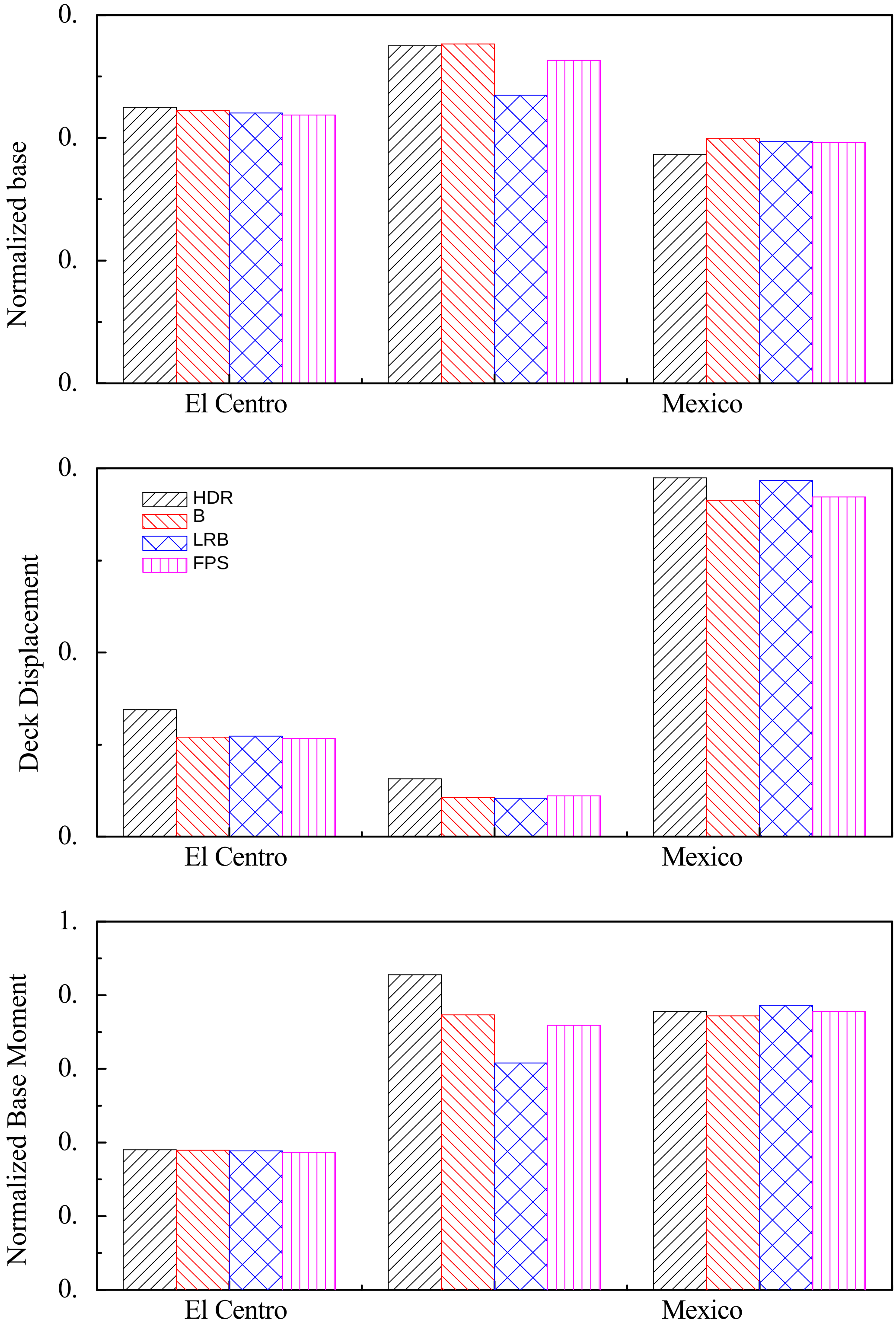

Figure 18. Comparison between different isolators.

Table 1. Evaluation criteria for the 1940 El Centro NS earthquake.

Criteria	HDRB	LRB	FPS	RFBI
J_1-Peak base shear	0.4500	0.4447	0.4406	0.4371
J_2-Peak shear at deck level	1.3489	1.3180	1.3386	1.3247
J_3-Peak base moment	0.3803	0.3788	0.3775	0.3733
J_4-Peak moments at deck level	0.7276	0.5993	0.6219	0.6064
J_5-Peak development of cable tension	0.2541	0.2514	0.2521	0.2524
J_6-Peak deck displacement	2.1533	1.6834	1.7012	1.6941
J_7-Normed base shear	0.2559	0.2498	0.2486	0.2468
J_8- Normed shear at deck level	1.4853	1.3496	1.2878	1.3140
J_9- Normed base moment	0.3951	0.3124	0.3043	0.3055
J_{10}- Normed moments at deck level	1.4862	0.9818	1.0206	1.0250
J_{11}- Normed development of cable tension	0.0324	0.0310	0.0296	0.0299
J_{12}-peak control force	0.0010	0.0017	0.0013	0.0013
J_{13}-maximum device stroke	1.4138	1.1053	1.1170	1.1123
J_{16}-number of control device	24	24	24	24

Table 2. Evaluation criteria for the 1985 Mexico City earthquake.

Criteria	HDRB	LRB	FPS	RFBI
J_1-Peak base shear	0.5502	0.5529	0.4697	0.5257
J_2-Peak shear at deck level	1.7238	1.5198	1.4789	1.4367
J_3-Peak base moment	0.8559	0.7468	0.6163	0.7120
J_4-Peak moments at deck level	0.9873	0.8384	0.7767	0.7256
J_5-Peak development of cable tension	0.0807	0.0943	0.0803	0.0825
J_6-Peak deck displacement	5.1358	3.4609	3.4113	3.7833
J_7-norm base shear	0.4233	0.4229	0.4273	0.4320
J_8-norm shear at deck level	1.5456	1.4056	1.2413	1.3519
J_9-norm base moment	0.6446	0.5524	0.5141	0.5628
J_{10}-norm moments at deck level	1.9384	1.3540	1.2643	1.3687
J_{11}-norm development of cable tension	0.0122	0.0125	0.0107	0.0110
J_{12}-peak control force	0.0005	0.0014	0.0009	0.0009

Table 2. Evaluation criteria for the 1985 Mexico City earthquake.(continued)

Criteria	HDRB	LRB	FPS	RFBI
J_{13} -max device stroke	2.5863	1.7429	1.7179	1.9052
J_{16} -number of control device	24	24	24	24

Table 3. Evaluation criteria for the 1999 Gebze earthquake.

Criteria	HDRB	LRB	FPS	RFBI
J_1 -Peak base shear	0.3724	0.3995	0.3941	0.3875
J_2 -Peak shear at deck level	2.0271	1.8683	1.9587	1.9430
J_3 -Peak base moment	0.7557	0.7440	0.7724	0.7637
J_4 -Peak moments at deck level	3.1459	3.0420	3.1802	3.1505
J_5 -Peak development of cable tension	0.3122	0.2927	0.3044	0.3043
J_6 -Peak deck displacement	9.8834	9.2612	9.8104	9.6986
J_7 -norm base shear	0.4179	0.3771	0.3998	0.3830
J_8 -norm shear at deck level	3.4097	2.5698	2.9559	2.9265
J_9 -norm base moment	1.3397	0.9783	1.1409	1.1188
J_{10} -norm moments at deck level	5.9746	4.1698	5.0107	4.9650
J_{11} -norm development of cable tension	0.0393	0.0303	0.0339	0.0334
J_{12} -peak control force	0.0030	0.0038	0.0034	0.0033
J_{13} -max device stroke	5.4189	5.0777	5.3788	5.3175
J_{16} -number of control device	24	24	24	24

Table 4. Maximum evaluation criteria for the entire three selected earthquake.

Criteria	HDRB	LRB	FPS	RFBI
J_1 -Peak base shear	0.5502	0.553	0.4697	0.526
J_2 -Peak shear at deck level	2.0271	1.868	1.9587	1.914
J_3 -Peak base moment	0.8559	0.747	0.7724	0.756
J_4 -Peak moments at deck level	3.1459	3.042	3.1802	3.069
J_5 -Peak development of cable tension	0.3122	0.293	0.3044	0.296
J_6 -Peak deck displacement	9.8834	9.261	9.8104	9.359
J_7 -norm base shear	0.4233	0.423	0.4273	0.432

Table 4. Maximum evaluation criteria for the entire three selected earthquake.(continued)

Criteria	HDRB	LRB	FPS	RFBI
J_8-norm shear at deck level	3.4097	2.570	2.9559	2.927
J_9-norm base moment	1.3397	0.978	1.1409	1.147
J_{10}-norm moments at deck level	5.9746	4.170	5.0107	4.964
J_{11}-norm development of cable tension	0.0393	0.031	0.0339	0.034
J_{12}-peak control force	0.0030	0.004	0.0034	0.005
J_{13}-max device stroke	5.4189	5.078	5.3788	5.131
J_{16}-number of control device	24	24	24	24

To investigate the robustness of the isolation systems on the seismic response of the bridge, the responses are obtained by varying important parameters of the isolation systems. The important parameters of the isolation systems are, damping ratio (ξ_b) for HDRB, normalized yield strength (F_0) for LRB and frictional coefficient (μ) for both FPS and R-FBI. The isolation time period (T_b) is common important parameter for all the isolators.

For the HDRB, the investigation is carried out by varying the parameter ξ_b from 5 to 30%. The variation of bearing displacement, base shear and base moment for different damping ratio of HDRB considering T_b = 3.5 sec is shown in Figure 10. It can be observed from Figure 10 that displacement as well as base moment response is decreasing with increase in damping ratio of the HDRB for all the three earthquakes considered. The isolator reduces the base shear response for the Mexico City (1985) earthquake significantly while the reduction for other two earthquakes is not significant. Hence from the Figure 10, it can be inferred that a higher amount of damping is beneficial in reducing the seismic responses of the benchmark cable-stayed bridge. Another study is carried out by varying the parameter T_b from 2.0 to 7.0 sec considering ξ_b equals to 15% and results are plotted in Figure 11. It is observed that isolator displacement increases with an increase in isolation period for all the three earthquakes. A trade-off between displacement of isolator and base shear response is observed. The isolation time period has little effect on base moment response for El Centro (1940), but it increases for Mexico City (1985) and decreases for Gebze (1999) earthquake with increase in T_b.

Figure 12 shows the variation of bearing displacement, base shear and base moment for different normalized yield strength (F_0) of LRB considering T_b = 3.5 sec. Investigation has been carried out for F_0 value from 0.05 to 0.3. It is evident from the figure that increase in F_0 values decreases bearing displacement and base moment responses significantly for Gebze (1999) earthquake but at the same time base shear increases. Base shear and base moment responses increase with increase in F_0 values for Mexico City (1985) earthquake. The variation of above responses for isolation period of 2.0 to 7.0 sec of LRB considering F_0 equal to 0.1 is demonstrated in Figure 13. It is found from this figure that increase in isolation time period has little effect on bearing displacement for El Centro (1940) and Mexico City (1985) earthquakes, but it increases significantly for Gebze (1999) earthquake. Base shear decreases significantly with an increase in isolation time period for Gebze (1999) earthquake. Base moment slightly decreases with an increase of isolation period for all three earthquakes considered.

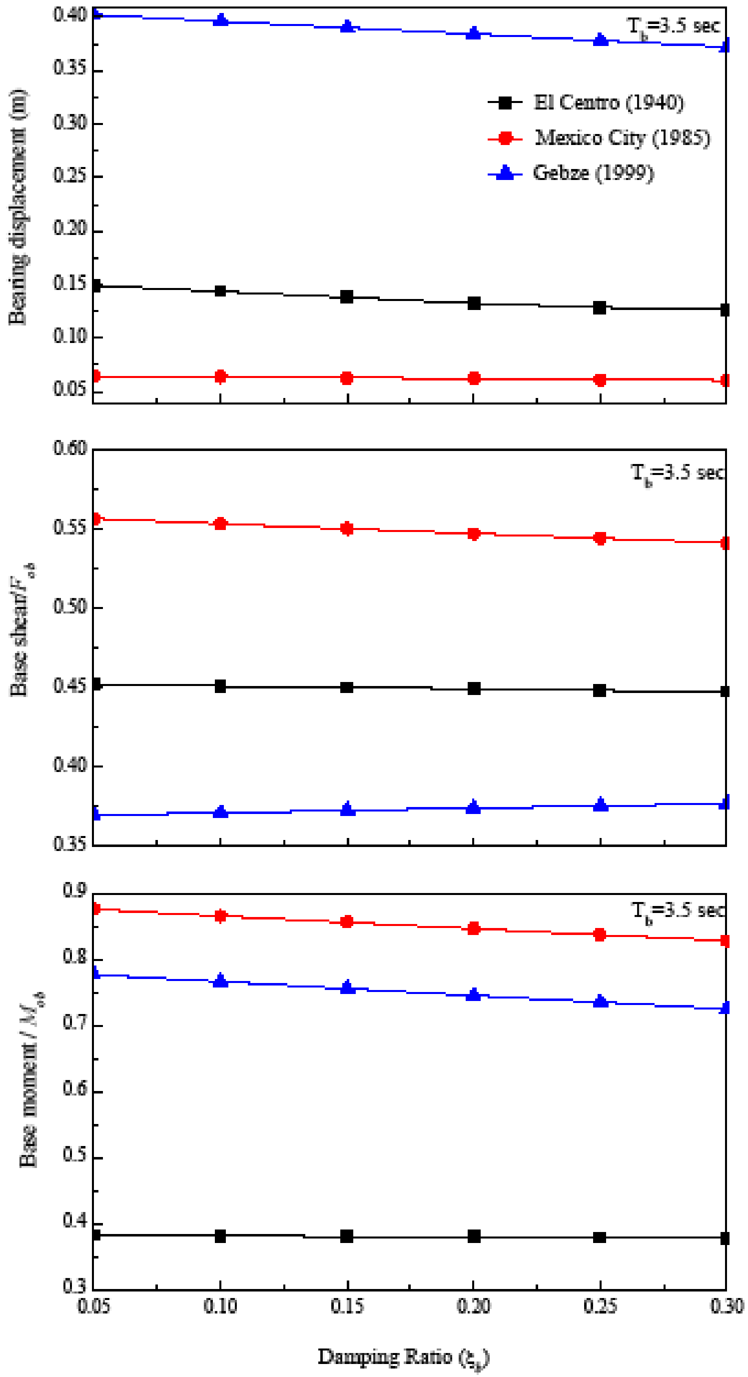

Figure 10. Effect of damping ratio of the HDRB on bearing displacement, peak base shear and peak base moment.

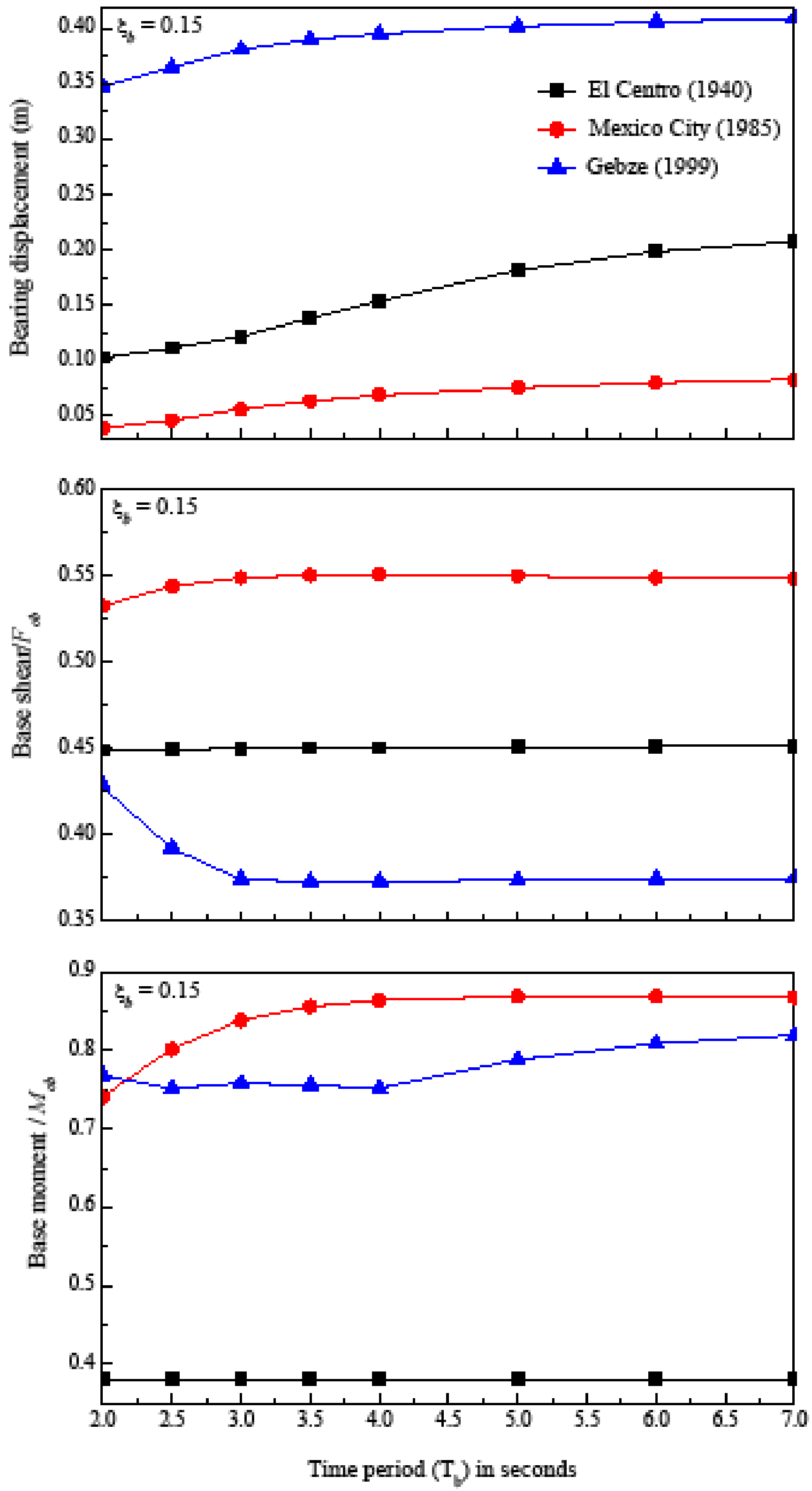

Figure 11. Effect of isolation time period of the HDRB on bearing displacement, peak base shear and peak base moment.

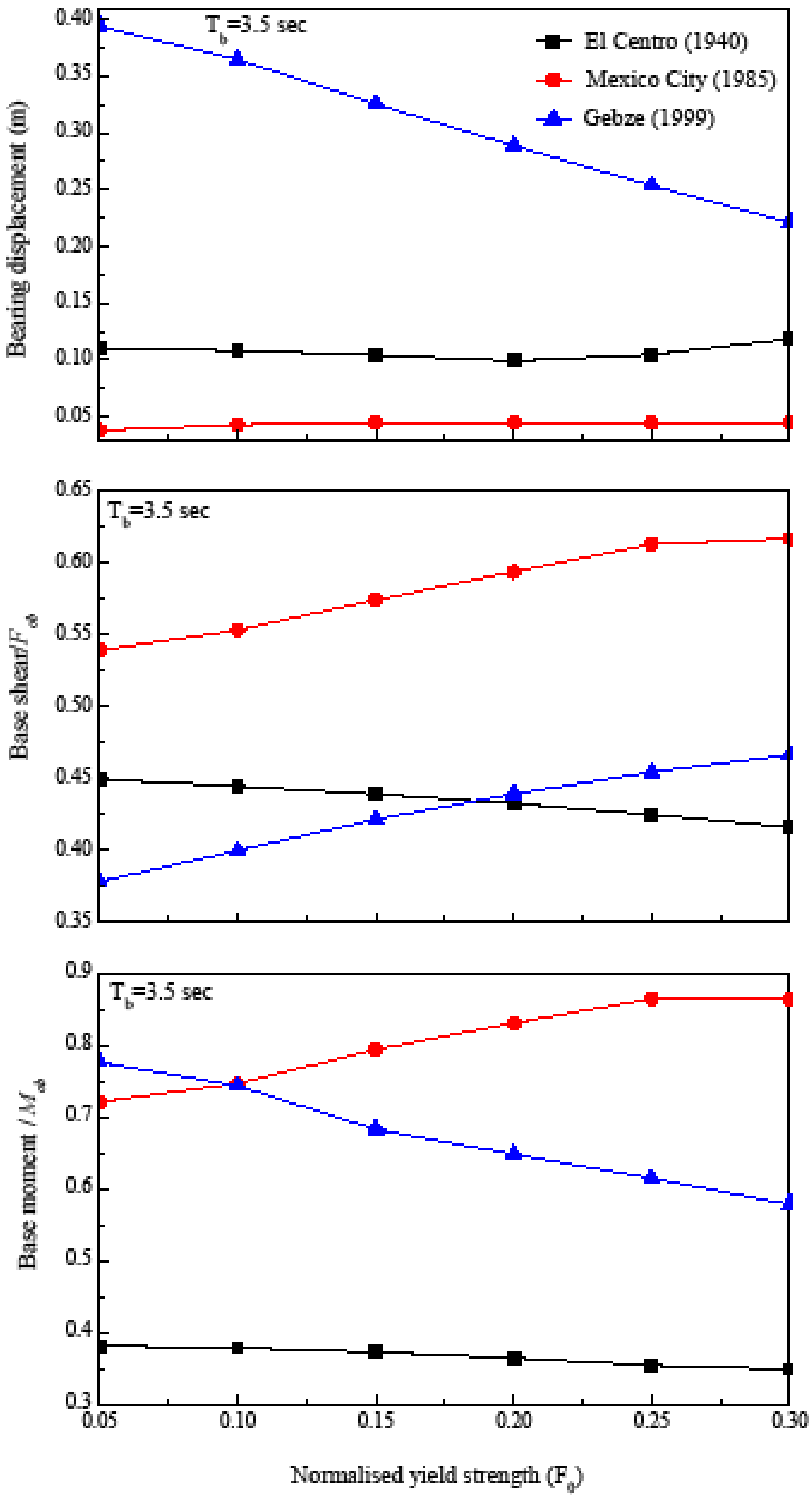

Figure 12. Effect of damping ratio of the LRB on bearing displacement, peak base shear and peak base moment.

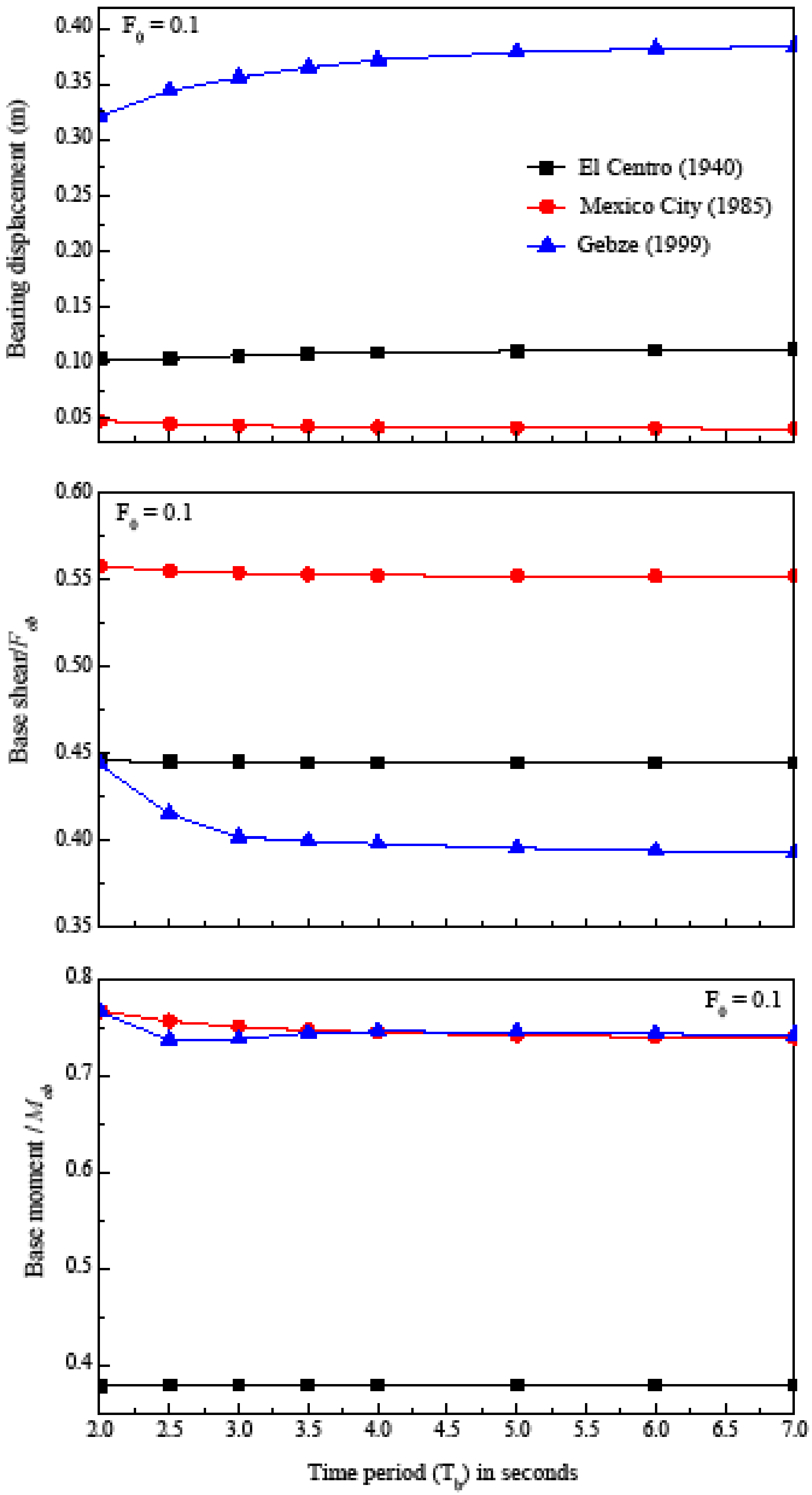

Figure 13. Effect of isolation time period of the LRB on bearing displacement, peak base shear and peak base moment.

The results of the parametric study performed on FPS for the variation of bearing displacement, base shear and base moment are presented in Figures 14 and 15. The influence of coefficient of friction (μ) of the FPS over the response of the benchmark bridge is investigated by varying it from 0.0 to 0.15. From Figure 14, it is revealed that increase in friction coefficient of FPS, decreases the bearing displacement response for Mexico City (1985) earthquake and Gebze (1999) earthquake significantly but has marginal effect for El Centro (1940) earthquake. With the increase in friction coefficient, base shear response decreases for El Centro (1940) earthquake but increases for Gebze (1999) earthquake and shows optimum value of μ for Mexico City (1985) earthquake. The base moment response decreases with the increase in μ for all the three earthquakes considered. It is observed from Figure 15 that bearing displacement increases and base shear decreases with increase in isolation time period of FPS for all the specified earthquakes.

The variation of bearing displacement, base shear and base moment for R-FBI, varying friction coefficient from 0.0 to 0.15, are presented in Figures 16 and 17. From Figure 16, it is observed that increase in friction coefficient of R-FBI, decrease the bearing displacement response for all the specified earthquakes, especially Gebze (1999) earthquake. With the increase in μ, base shear response decreases for El Centro (1940) but increases for Gebze (1999) and shows optimum value of μ for Mexico City (1985) earthquake. The base moment response decreases with the increase in μ for all the three earthquakes considered but again shows optimum value of μ for Mexico City (1985) earthquake. It is observed from Figure 17 that variation of responses is not significant with increase in isolation time period of R-FBI for all the specified earthquakes.

The results of the numerical study exhibit that for the flexible structure like cable-stayed bridge, which is already having natural isolation by virtue of its large fundamental period, nevertheless, the seismic isolation is found very much effective in reducing seismically induced forces with manageable deck displacement. It is also observed that parameters of the isolators have significant effect on the response of the bridge. Higher values of ξ_b, F_0 and μ than the normal is beneficial for securing the displacement and base shear response of the bridge. Among the three isolators, HDRB produces larger displacement than the other three isolators for all the three earthquakes but most effective in controlling the base shear response of the Gebze (1999) earthquake. From the parametric study, it is found that LRB is more robust than other isolators.

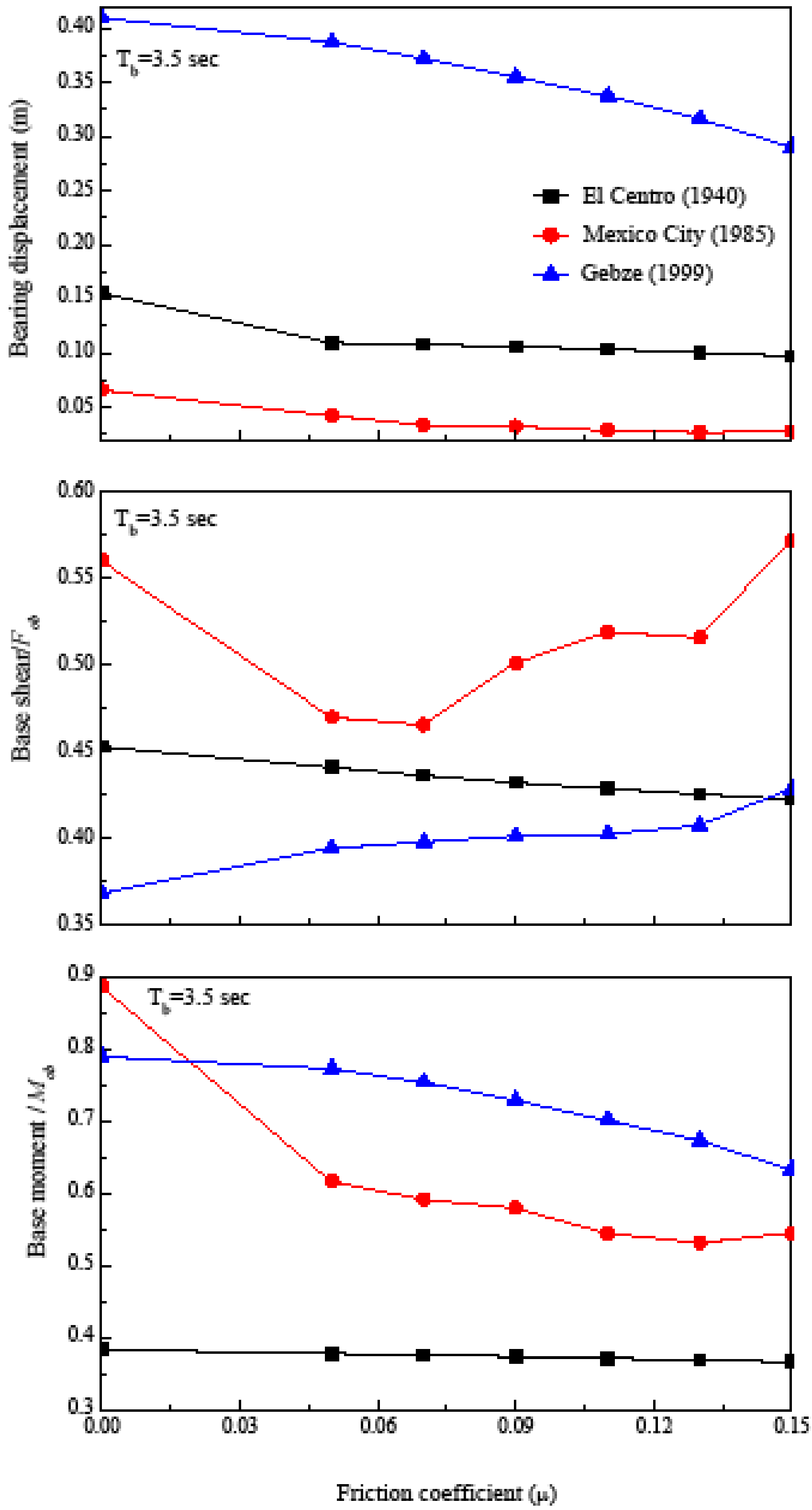

Figure 14. Effect of friction coefficient of the FPS on bearing displacement, peak base shear and peak base moment.

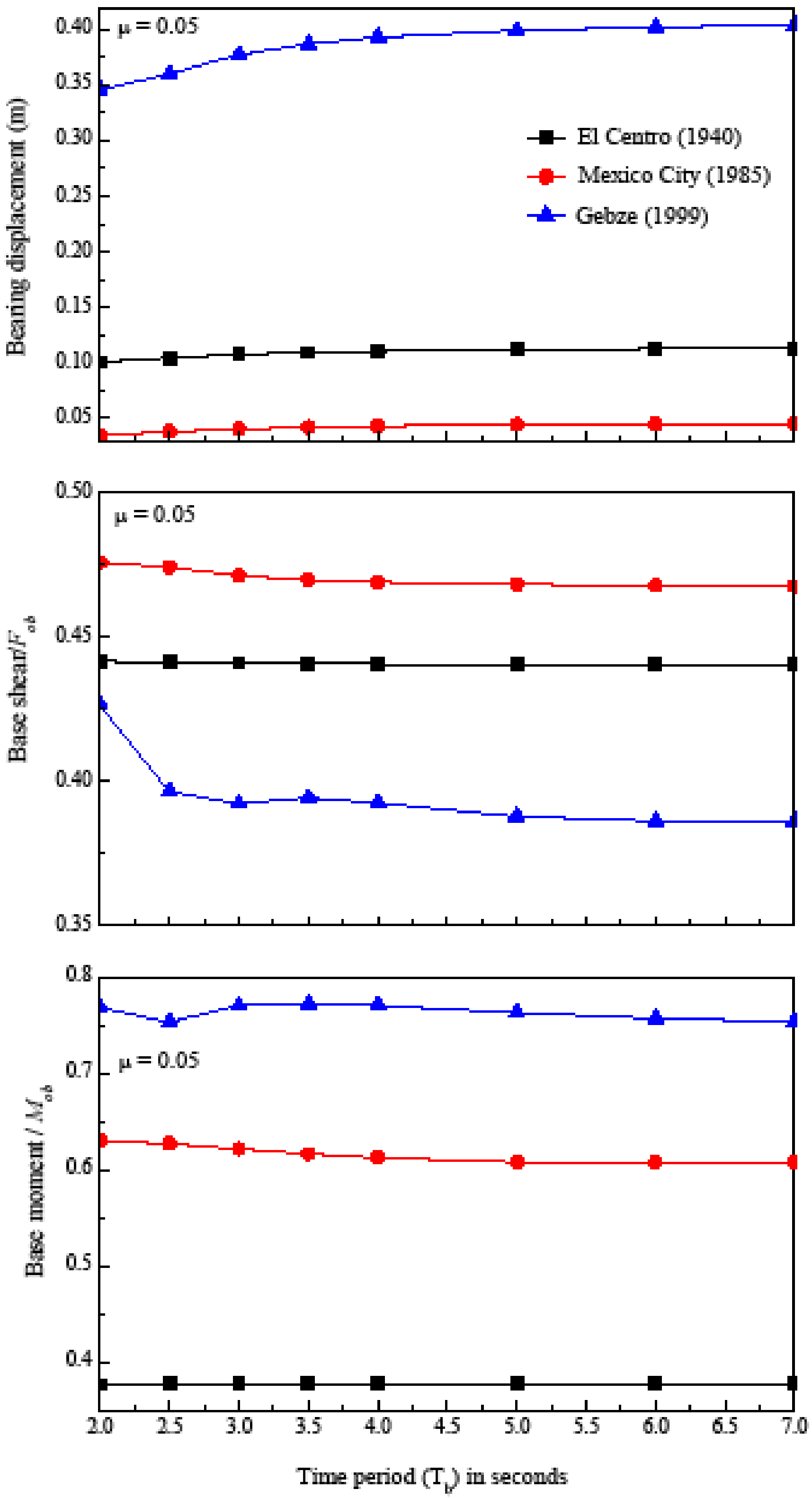

Figure 15. Effect of isolation time period of the FPS on bearing displacement, peak base shear and peak base moment.

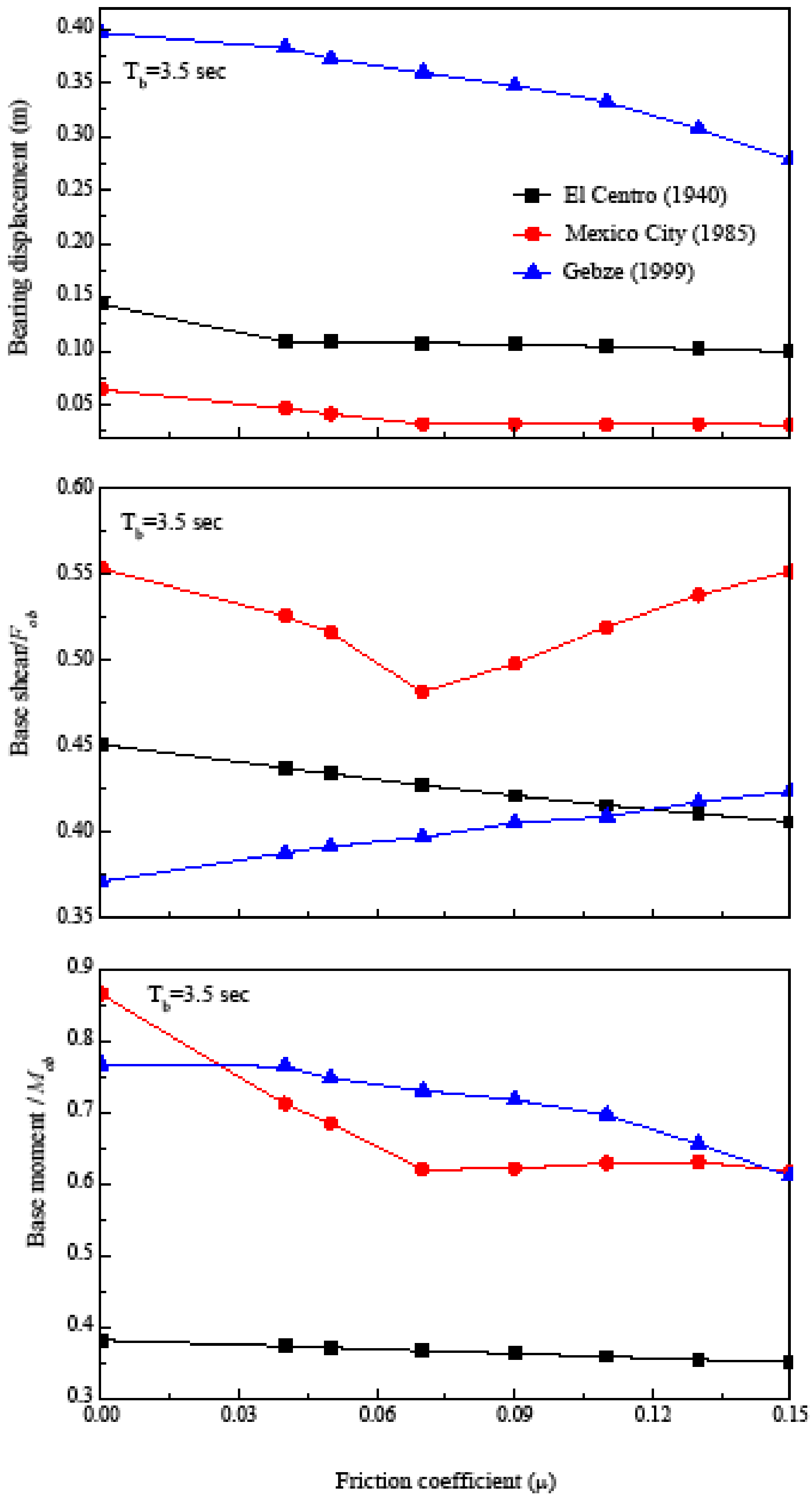

Figure 16. Effect of friction coefficient of the R-FBI on bearing displacement, peak base shear and peak base moment.

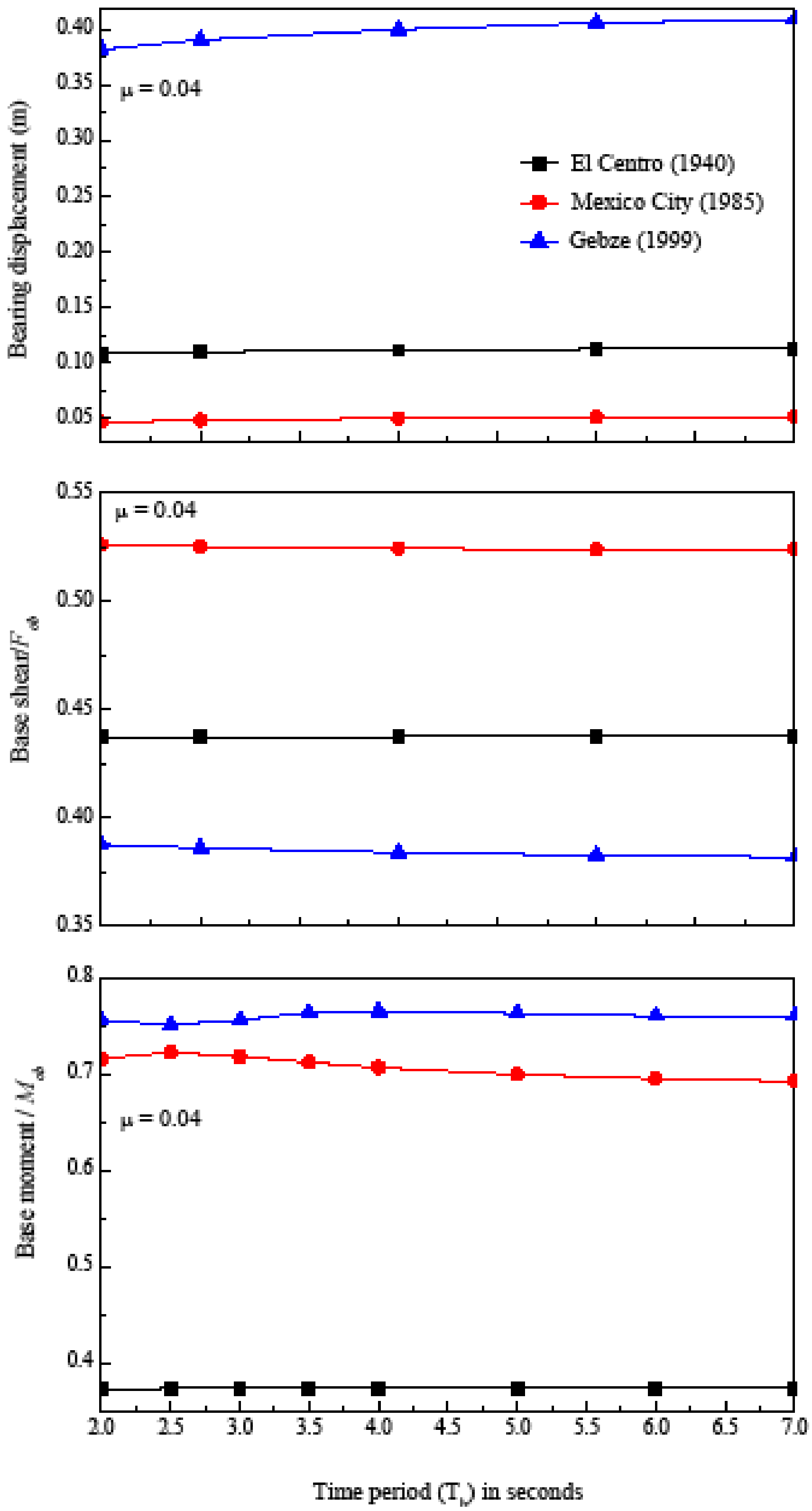

Figure 17. Effect of isolation time period of the R-FBI on bearing displacement, peak base shear and peak base moment.

6. Conclusions

In this study, an attempt is made to compare the effectiveness of different seismic isolators for benchmark cable-stayed bridge. The performance of the bridge under different isolators is investigated and the results are tabulated in the form of evaluation criteria's mentioned in the benchmark problem for direct comparison. Parametric studies have been carried out by varying the important parameters of each isolator. Based on the investigation performed on the seismic response control of the bridge, the following conclusions are drawn:

1. Despite being a flexible structure, significant seismic response reduction of the bridge can be achieved by installing HDRB, LRB, FPS and R-FBI in the benchmark cable-stayed bridge.
2. Reduction in the base shear response of the towers is achieved about 45 to 70% for all the types of specified isolator and earthquake ground motion.
3. The reduction of the seismic responses depends on the types of isolator as well as types of earthquake ground motions.
4. Increase in damping ratio of HDRB, normalized yield force of LRB and friction coefficient of FPS and R-FBI decrease the seismically induced forces of the bridge. On the other hand, isolation time period of the isolators has a significant effect on the seismic responses but again depends on the types of earthquake ground motion.
5. Comparing the values of evaluation criteria tabulated, it can be deduced that LRB is more robust than the other isolators
6. The performance of R-FBI is found to be better than that of HDRB and FPS.

References

[1] Dyke, S. J., Caicedo, J. M., Turan, G., Bergman, L. A., and Hague, S. 2003. Phase I benchmark control problem for seismic response of cable-stayed bridges. *Journal of Structural Engineering*, ASCE, 129:857-872.

[2] Ali, H. M., and Abdel-Ghaffar, A. M. 1994. Seismic energy dissipation for cable-stayed bridges using passive devices. *Earthquake Engineering and Structural Dynamics*, 23:877-893.

[3] Iemura, H., and Pradono, M. H. 2003. Application of pseudo-negative stiffness control to the benchmark cable-stayed bridge. *Journal of Structural Control*, 10:187-203.

[4] Park, K., Jung, H., and Lee, I. 2003. Hybrid control strategy for seismic protection of benchmark cable-stayed bridge. *Engineering Structures*, 25:405-417.

[5] Jung, H. J., Park, K. S., Spencer, Jr, B. F. and Lee, I. W. 2004. Hybrid seismic protection of cable-stayed bridge. *Earthquake Engineering and Structural Dynamics*, 33:795-820.

[6] Bontempi, F., Casciati, F., and Giudici, M. 2003. Seismic response of a cable-stayed bridge: active and passive control systems (Benchmark Problem). *Journal of Structural Control*, 10:169-185.

[7] He, W., and Agrawal, A. K. 2007. Passive and hybrid control systems for seismic protection of a benchmark cable-stayed bridge. *Structural Control and Health Monitoring*, 14:01-026.

[8] Jangid, R. S. 2002. Parametric study of base-isolated structures. *Advances in Structural Engineering*, 5:113-122.

[9] Naeim, F., and Kelly, J. M. 1999. "*Design of seismic isolated structures*". John Wiley & Sons, Inc. Canada.

[10] Robinson, W. H., and Tucker, A. G. 1977. A lead-rubber shear damper. *Bulletin of New Zealand National Society for Earthquake Engineering*, 8:187-191.

[11] Robinson, W. H. 1982. Lead-rubber hysteretic bearings suitable for protecting structures during earthquakes. *Earthquake Engineering and Structural Dynamics*, 10:593-604.

[12] Wen, Y. K. 1976. Method for random vibration of hysteretic systems. *Journal of Engineering Mechanics*, ASCE, 102:249-263.

[13] Zayas, V. A., Low, S. S., and Mahin, S. A. 1990. A simple pendulum technique for achieving seismic isolation. *Earthquake Spectra*, 6:317–333.

[14] Jangid, R. S. 2005. Computational numerical models for seismic response of structures isolated by sliding systems. *Structural Control and Health Monitoring*, 12:117-137.

[15] Mostaghel. N., and Khodaverdian, M. 1987. Dynamics of resilient-friction base isolator (R-FBI). *Earthquake Engineering and Structural Dynamics*, 15:379-390.

[16] SIMULINK. The Math Works Inc. 1997. Natick, Massachusetts.

[17] MATLAB. The Math Works Inc. 2002. Natick Massachusetts.